Coupled Level set moment of fluid method for simulating multiphase flows

Anirudh Asuri Mukundan, Thibaut Ménard, Alain Berlemont, Jorge César C Brändle de Motta

Coupled Level set moment of fluid method for simulating multiphase flows

Anirudh Asuri Mukundan*, Thibaut Ménard, Alain Berlemont, Jorge César Brändle de Motta
CNRS UMR6614-CORIA, Rouen, France
*Corresponding author: anirudh.mukundan@coria.fr

Abstract

A coupled level set moment of fluid (CLSMOF) method for numerical simulation of multiphase flows is presented in this paper. This numerical method of liquid/gas interface capture is a hybrid of classical moment of fluid (MOF) method and coupled level set volume of fluid (CLSVOF) method. In this CLSMOF method, MOF interface reconstruction is used only for the under-resolved liquid structures while the level set function is used for the interface reconstruction for the resolved structures. This method combines the advantages of accurate capture of under-resolved liquid strucutres from MOF method and sharp interface representation by the level set function. The results presented in this paper demonstrates the ability and accuracy of the CLSMOF method to be as high as that of the MOF method while incurring relatively less computational expense. Finally, the application of CLSMOF method to simulation of turbulent diesel jet yeilded a very satisfactory volume conservation.

Keywords

CLSMOF, atomization, CLSVOF, phase centroid, DNS

Introduction

The atomization process of the liquid fuel injected in aircraft engines plays a pivotal role in its subsequent combustion and pollutants formation. In order to meet the stringent emission regulation norms and increase engine efficiency, it is imperative to study the breakup process of the liquid fuel. The experimental investigations of fuel breakup has been able to generate lots of database of measurements but these pertain to the far downstream of the liquid fuel disintegration process. The access to the dense spray region is restricted and not much data is available. This motivates the development of novel and accurate numerical methods for simulating the atomization process on large supercomputers. The important requirement for these numerical methods is least numerical error and less computational expenses thus not enforcing load on even powerful supercomputers available today [1].

The liquid fuel atomization process is a complex, turbulent, multiphase, and multiscale flow process. Within the context of numerically simulations of multiphase flows, Navier-Stokes equations are solved. The critical aspect in such simulations is the accurate capture of the liquid/gas interface. The accuracy of interface capture is an important factor since the liquid volume contained within the interface has a direct impact on the computation of density. Any discrepancy in the computation of density can have a detrimental effect on the computation of velocity when solving the Navier-Stokes equations. Thus, to this end, over the past decades, there have been a variety of numerical methods developed for accurate capturing of liquid/gas interface. Of these, the two family of methods are volume of fluid (VOF) and level set (LS) methods. On one hand, the VOF method uses the amount of liquid fuel in each computational cell in the numerical domain to determine the location and orientation of the interface. A variety of VOF-variant methods exist in the literature [2–5]. On the other hand, the LS method [6–8] has an implicit interface representation and the equation of the signed distance level set function is expressed in a geometrically easy way. This facilitates in computation of geometrical quantites such as interface curvature. The main drawback of this method is the inability to conserve liquid mass. To alleviate these limitations, a coupled level set volume of fluid (CLSVOF) method [9–11] had been developed. Although this method had been shown to be better than the VOF and LS methods, it can still fail in computation of geometric quantities especially for under-resolved liquid structures.

To this end, moment of fluid (MOF) method was developed by Dyadechko and Shashkov [12]. This method uses zeroth and first moments of liquid volume fraction in reconstructing the liquid/gas interface. It has been shown by Jemison et al [13] that MOF method performs better than CLSVOF method especially in capturing sharp under-resolved and thin liquid structures. In our group, a similar conclusion has been reached [14, 15]. The interface reconstruction technique of MOF method involves solving a local non-linear optimization problem which can potentially become computationally expensive as the optimization depends severely on the initial guess.

In order to mitigate this bottleneck, we have developed a coupled level set moment of fluid (CLSMOF) method in our in-house code ARCHER. Within our work, we have developed CLSMOF method as a hybrid between MOF and CLSVOF method in which each computational cell is assigned a decision between MOF and CLSVOF methods for interface reconstruction. The motivation is that MOF method will be used for interface reconstruction only when an under-resolved liquid structure is detected. In order to detect such structures, we have proposed an criterium called *interface resolution quality* (IRQ) that distinguishes the resolved from the under-resolved liquid structures.

This paper is organized as follows. First, the governing Navier-Stokes equations solved in ARCHER are presented. This is followed by the presentation of the CLSMOF method. Results from various canonical tests and simulation of turbulent diesel jet are then presented demonstrating the ability and accuracy of CLSMOF method. Finally, concluding remarks are drawn based on the presented results.

Governing Equations

The solver used in this study is ARCHER, whose capabilities are described extensively in multiple works [6, 10, 16]. This solver is structured, parallel and developed for direct numerical simulations (DNS) of complex and turbulent multiphase flows with the application to study primary breakup of liquid fuel jet. A staggered variable configuration is used with central finite difference scheme for least numerical dissipation.

The pressure and velocity fields describing the flow are obtained by solving the incompressible Navier–Stokes equations. The following form of the Navier–Stokes equations are solved in ARCHER:

$$\boldsymbol{\nabla} \cdot \boldsymbol{u} = 0, \tag{1}$$

$$\frac{\partial \rho \boldsymbol{u}}{\partial t} + \boldsymbol{\nabla} \cdot (\rho \boldsymbol{u}\, \boldsymbol{u}) = -\boldsymbol{\nabla} P + \boldsymbol{\nabla} \cdot (2\mu \boldsymbol{D}) + \boldsymbol{B}, \tag{2}$$

where $\boldsymbol{u}$ is the velocity field, P is the pressure field, μ is dynamic viscosity, ρ is density, $\boldsymbol{D}$ is the strain rate tensor given as $\boldsymbol{D} = \frac{1}{2}(\boldsymbol{\nabla u} + (\boldsymbol{\nabla u})^T)$, and $\boldsymbol{B}$ is the sum of the body and surface tension forces. $\boldsymbol{B} = \boldsymbol{B}_{\mathrm{b}} + \boldsymbol{B}_{\mathrm{st}}$ where $\boldsymbol{B}_{\mathrm{b}}$ is the force due to gravity and $\boldsymbol{B}_{\mathrm{st}}$ is the force due to surface tension which is given as $\boldsymbol{B}_{\mathrm{st}} = \sigma\kappa\delta_I \boldsymbol{n}$. σ represent the surface tension, κ is the curvature of the interface computed using the level set function ϕ as

$$\kappa = -\boldsymbol{\nabla} \cdot \frac{\nabla \phi}{\|\nabla \phi\|_2}, \tag{3}$$

and δ_I is the Dirac delta function centered on it. A consistent mass and momentum flux computation [16] is employed.

A projection method as described in Ménard et al [10] is employed for solving Equations (1) and (2). A 2^{nd} order central difference scheme is employed for discretization of the spatial derivatives to avoid any dissipation. However, the convection term is discretized using 5^{th} order WENO scheme to ensure a robust behavior of the solution. A consistent mass and momentum flux computation [16] is employed. The viscous term is discretized following the method described in Sussman et al [17]. Ghost Fluid Method (GFM) [18] is employed for the spatial discretization of the Poisson equation for taking into account the force due to surface tension as a pressure jump. The resulting linear system of symmetric and positive definite matrix with five diagonals is solved using multigrid algorithm for preconditioning a conjugate gradient (CG) method [6]. The temporal derivatives in this study are discretized using one-step forward Euler scheme.

CLSMOF Method

In this section, we first briefly summarize the coupled level moment of fluid (CLSMOF) method employed for liquid/gas interface capturing within the context of multiphase flows. Then the numerics behind the CLSMOF interface reconstruction and advection are presented. Finally, a criteria for distinguishing resolved and under-resolved interface is presented.

Within the context of multiphase flows, it is imperative to accurately capture the liquid/gas interfaces. To this end, we have developed CLSMOF interface reconstruction method. This method is a combination of classical moment of fluid (MOF) [14, 15] and coupled level set moment of fluid (CLSVOF) [10] methods. This way, it is possible to combine the advantages of both methods: accurate capture of under-resolved liquid droplets from MOF and sharp interface representation from LS methods. The objective is to use the computationally more expensive MOF method only for reconstructing under-resolved liquid structures.

MOF Method

MOF method is a superset of conventional volume of fluid (VOF) method. MOF method tracks both liquid volume fraction (zeroth moment of liquid volume) and phase centroids (first moment of liquid volume) in each mixed computational cell (cell with non-zero liquid volume fraction) in order to numerically reconstruct the interface. A piecewise linear interface calculation (PLIC) method is used for reconstructing the interface. Thus, the equation of the reconstructed interface plane (line in 2D) is given as $ax + by + cz + d = 0$ where interface normal $\boldsymbol{n} = [a, b, c]^T$. The reconstruction of original/reference interface means determining the components of interface normal $\boldsymbol{n}$ and shortest distance of interface from cell center d. In MOF method, we find these two quantities by satisfying volume conservation (Equation (4)) and least centroid defect (Equation (5)). The centroid defect is defined as the distance between the coordinates of the phase centroids of the reference and actual/reconstructed interface. The two conditions are:

$$\mid F^{\mathrm{ref}} - F^{\mathrm{act}}(\boldsymbol{n}, d) \mid = 0, \text{ and} \tag{4}$$

$$E^{\mathrm{MOF}}(\boldsymbol{n}, d) = \min_{\text{Eq. (4) holds}} \left\| \boldsymbol{x}^{\mathrm{ref}}_{\mathrm{COM}} - \boldsymbol{x}^{\mathrm{act}}_{\mathrm{COM}}(\boldsymbol{n}, d) \right\|_2. \tag{5}$$

where F represent liquid volume fraction and x_{COM} is the liquid phase centroid. All the variables containing the superscript "ref" represents the variables pertaining to the original (reference) interface while those containing the superscript "act" represents the variables pertaining to the reconstructed (actual) interface. The reference interface is chosen for a fluid (either liquid/gas) based on the farthest distance of its centroid from the cell center x_{C_Ω} (where C_Ω is a computational cell inside the domain Ω), i.e.,

$$\text{Reference fluid} = \begin{cases} \text{liquid}, & \left\| \boldsymbol{x}^{\mathrm{ref}}_{\mathrm{COM,liq}} - \boldsymbol{x}_{C_\Omega} \right\| > \left\| \boldsymbol{x}^{\mathrm{ref}}_{\mathrm{COM,gas}} - \boldsymbol{x}_{C_\Omega} \right\| \\ \text{gas}, & \text{otherwise.} \end{cases} \tag{6}$$

Thus, the centroid defect is minimized for the phase with the minimum volume in the cell. The rationale behind this approach is that, the interface orientation has highest sensitivity to the centroid defect of the phase with least volume. For the purpose of illustration, Figure 1 shows a typical computational cell in 2D with the reference and reconstructed interfaces based on liquid as reference fluid. The parameter d is computed as a result of satisfying

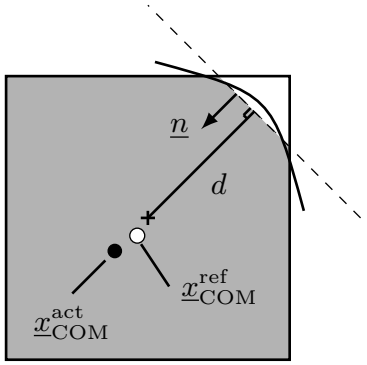

Figure 1. Computational cell with reference (solid line) and reconstructed (dashed line) interfaces and liquid centroid.

the volume conservation condition (Equation (4)) upto the machine precision using Newton-Raphson method. The interface normal $\boldsymbol{n}$ is obtained from minimizing the centroid defect E^{MOF} using Gauss-Newton minimization method. It is to be mentioned that this minimization algorithm finds local minima and not the global minima. The reference liquid volume fraction F is advected by a directionally split algorithm described in [19] and the reference liquid and gas phase centroids are advected using a directionally split Eulerian Implict-Lagrangian Explicit (EI-LE) scheme. For more details, the readers are referred to Asuri Mukundan et al [14].

CLSVOF Method

The coupled level set volume of fluid (CLSVOF) method of Ménard et al [10] is used for obtaining the level set function for interface capturing in our solver.

Interface Resolution Quality

The main idea of the CLSMOF method development is to use MOF only when it is necessary. This necessity is driven by presence of under-resolved liquid structures which are smaller in size than the employed mesh resolution. Thus, it is required to find and distinguish resolved and under-resolved liquid structures from one another. To this end, we propose a criteria called *interface resolution quality* (IRQ) which is expressed as

$$\mathrm{IRQ} = \frac{1}{\Delta x \mid \kappa \mid}, \tag{7}$$

where Δx is the mesh spacing and κ is the liquid/gas interface curvature. The threshold value of IRQ determines which of the liquid structures in the domain are resolved and which are under-resolved. Based on the literature [1, 20], we decided to use the threshold value of 2.0 for IRQ. This means, for any computational cell containing a liquid phase and has a value of IRQ less than 2.0 (correspondingly, less than 8 cells along the liquid structure effective spherical diameter) would be treated as under-resolved liquid cell structure, thus, MOF will be employed for interface reconstruction. For all other IRQ values, the level set function from CLSVOF method will be used for interface reconstruction. It is to be remarked that Jemison et al [13] used a similar criteria with a higher threshold value in their work.

Results and Discussion

In this section, we present the results from using the CLSMOF method for capturing the liquid/gas interface for various tests. The first presented test is the deformation of 3D droplet in a solenoidal velocity field in which a spherical liquid droplet undergo deformation forming a thin sheet. Then, we move to the test on the Rayleigh-Taylor instability to assess the accuracy of the interface capture for thin filaments. Finally, we demonstrate the ability of CLSMOF method for real flows by capturing the liquid/gas interface for turbulent diesel jet.

Deformation of a spherical droplet

In this test, an initially spherical liquid droplet of radius 0.15 located with its center at $(0.35, 0.35, 0.35)$ in a $[1 \times 1 \times 1]$ domain is made to undergo sever deformation. The velocity field prescribed in this test is given as

$$u(x, y, z, t) = 2\sin^2(\pi x)\sin(2\pi y)\sin(2\pi z)\cos(\pi t/3) \tag{8}$$

$$v(x, y, z, t) = -\sin(2\pi x)\sin^2(\pi y)\sin(2\pi z)\cos(\pi t/3) \tag{9}$$

$$w(x, y, z, t) = -\sin(2\pi x)\sin(2\pi y)\sin^2(\pi z)\cos(\pi t/3) \tag{10}$$

where x, y, z are spatial coordinates and t is the simulation time. With this time reversing velocity field, an initial spherical interface is stretched to form a thin sheet at $t = 1.5$ and reverses back to its original spherical shape at

$t = 3.0$. The objectives for an interface reconstruction method in this test case are: 1) to accurately capture the thin sheet/membrane without any holes in them; and, 2) preserve the shape of the sphere at the end of the simulation. Five different mesh resolutions have been used for simulating this test case on CRIANN's Myria supercomputer with a constant CFL number of 0.5. The error in the accuracy of the interface reconstruction at $t = 3$ is measured using symmetric difference area error [12, 13]. This error is expressed as

$$E_{\text{symm}} = \sum_{i,j,k} \int_{C_{\Omega_{i,j,k}}} \Big| H(\boldsymbol{n} \cdot (\boldsymbol{x} - \boldsymbol{x}_{\boldsymbol{C_\Omega}}) + d) - H(\phi_{\text{exact}}(\boldsymbol{x})) \Big| d\boldsymbol{x} \tag{11}$$

where ϕ_{exact} is the level set function of the exact interface determined analytically, H is the Heaviside function, and C_Ω refers to a computational cell in the domain Ω. It measures the area between the reference and actual/recontructed interface as shown in Figure 2.

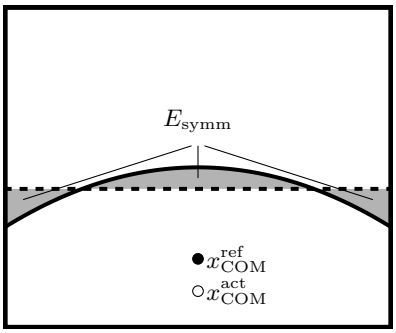

Figure 2. Illustration of symmetric difference area error shown as grey regions along with reference interface (solid line) and actual/reconstructed interface (dashed line).

Figure 3 shows the phase interfaces corresponding to zero-level isocontour of level set function for start, middle and end of simulations for CLSMOF, MOF, and CLSVOF methods. In Figures 3a to 3c, the coloring is based on whether the interface has been reconstructed using MOF method (red regions) or CLSVOF method (blue region) for that particular time instant. Just per the definition of the IRQ (c.f. Equation (7)), the MOF method is being executed at the high curvature regions where there is significant change in the direction of interface unit normal between adjacent cells. Furthermore, the MOF method is used for reconstructing the membrane that are few cells thick even though the curvature in this region is nearly zero. The reason for such a behavior in our results stems from the fact that, in our solver, the curvature is computed with a 3-point stencil using the level set function which is corrected based on the liquid volume fraction determined from the interface reconstruction method. Since the membrane is few cells thick, the stencil scheme does results to low curvature values thereby inducing MOF to be used over CLSVOF method.

On observing Figures 3d to 3f and Figures 3g to 3i, we can see that albeit CLSVOF method is able to capture the thin membrane, the final shape is not well preserved in comparison to the MOF and CLSMOF method. This point is also proved by the quantitative assessment of the symmetric difference error shown in Figure 4a. The errors for the CLSVOF methods are consistently higher than that of the MOF and CLSMOF methods especially for the less number of mesh cells in the domain. All the methods are seen to exhibit second-order convergence in the symmetric difference error. Although solving the local non-linear optimization using Gauss-Newton method can be expensive for MOF method, it is proved otherwise for CLSMOF method as seen in Figure 4b. For all the mesh resolutions, the average CPU time taken per timestep (defined as ratio of product of total wall time and number of processors to that of the total number of time steps) is seen to be less than the MOF method, of about 36% less time per time step for $N_x = 128$. Moreover, two distinct observations can be made from Figure 4b: first, the time taken for the CLSMOF method is almost the same as that for the MOF method for smaller value of N_x due to the fact that majority of the interface is under-resolved; second, the time taken for the CLSMOF method approaches that of CLSVOF method with the increase in N_x since the interface becomes resolved thereby leading to usage of level set for interface reconstruction under the umbrella of CLSMOF method.

Rayleigh-Taylor Instability

This test is performed to assess the coupling between the CLSMOF method and our flow solver for Navier-Stokes equations. The setup of this case in this paper follows the work of Desjardins and Pitsch [21]. In this test case, a 1×4 domain is considered containing two fluid phases about each other that are separated by an interface. This interface is defined by the zero value of the level set given as

$$\phi(x, y) = y + A\cos(2\pi x) \tag{12}$$

where $A = 0.05$ is chosen for this test case. The density of the top fluid (denoted as fluid 1) is $\rho_1 = 1.225$ while that of the bottom fluid (denoted as fluid 2) is $\rho_2 = 0.1694$. The dynamic viscosities of the two fluids are same $\mu_1 = \mu_2 = 0.00313$. The surface tension is taken as $\sigma = 0.1337$. Periodic boundary condition is considered along $x-$direction and wall boundary condition along $y-$direction. Five different mesh resolutions are considered ranging

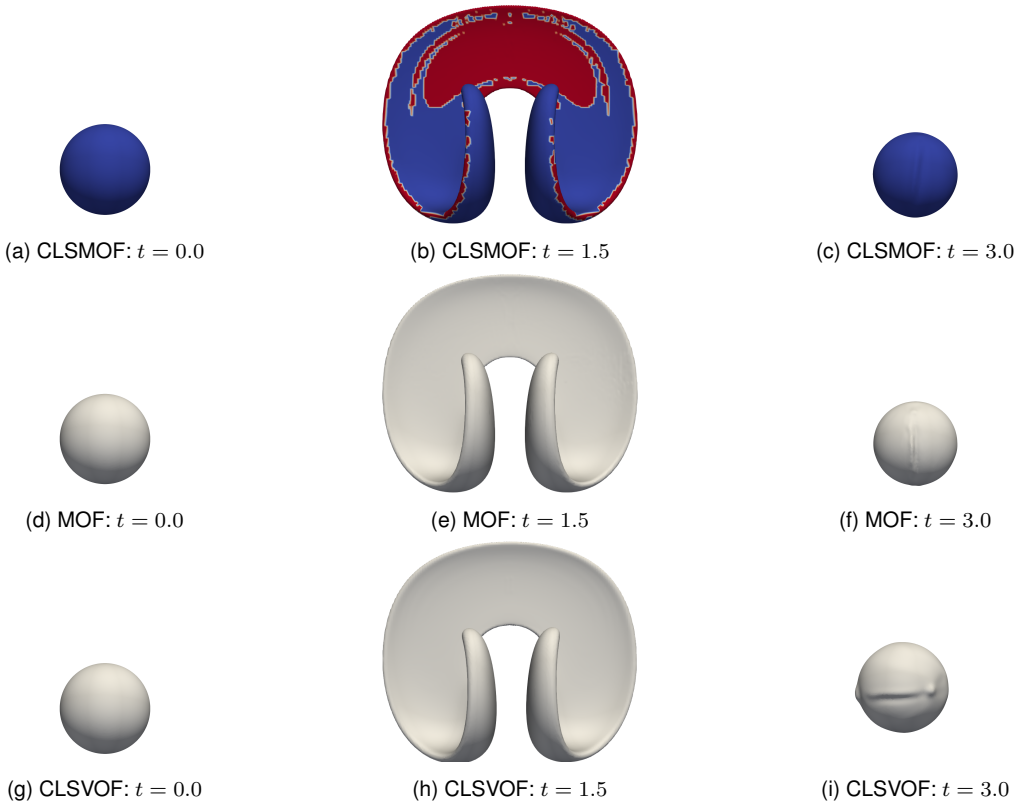

(a) CLSMOF: $t = 0.0$ (b) CLSMOF: $t = 1.5$ (c) CLSMOF: $t = 3.0$

(d) MOF: $t = 0.0$ (e) MOF: $t = 1.5$ (f) MOF: $t = 3.0$

(g) CLSVOF: $t = 0.0$ (h) CLSVOF: $t = 1.5$ (i) CLSVOF: $t = 3.0$

Figure 3. Phase interface of spherical droplet deformation for 192^3 grid. (a)–(c): red regions (MOF) and blue regions (CLSVOF).

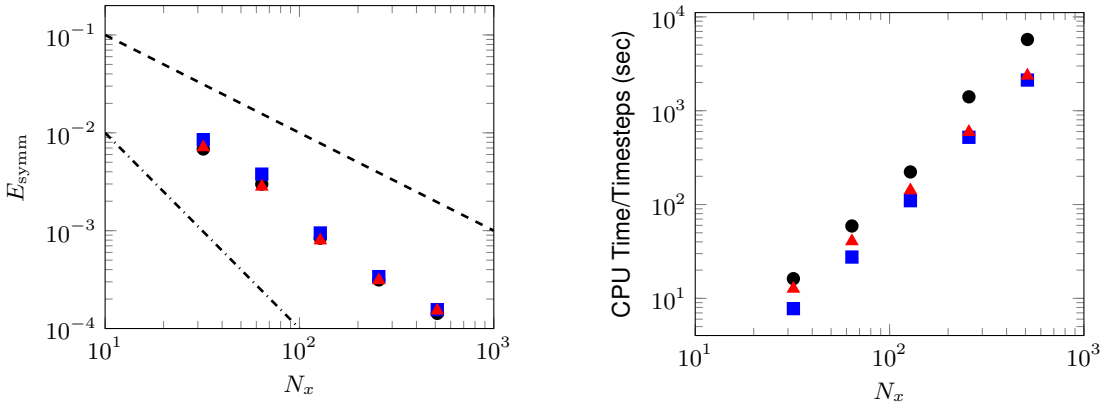

(a) Symmetric difference error

(b) Average CPU time per timestep

Figure 4. Symmetric difference error (a) and average CPU time per timestep (b) for spherical droplet deformation: MOF (●); CLSVOF (■); CLSMOF (▲); 1^{st} order convergence: (- - -); 2^{nd} order convergence: (-·-·-).

from 32×128 to 512×2048. The test case is run upto a physical time of $t = 1.2$. With the ability of the CLSMOF method over the MOF and CLSVOF methods shown in the above test, we present here the results only from the CLSMOF method.

Figure 5 shows the time evolution of the phase interface shape for the Rayleigh-Taylor instability test using 512×2048 mesh resolution. The results are in good agreement with that from the work of Desjardins and Pitsch [21] which was performed using a spectrally refined interface method.

Figure 6 shows the fluid phase interfaces for all mesh resolutions for the time steps $t = 1.0, 1.1, 1.2$. The arrow in these figures indicates the increasing mesh resolutions considered in this work for this test case. The depth until which the fluid 1 goes into the fluid 2 is defined as the spike penetration within this work. The value of the spike penetration for the mesh resolution 512×2048 is used as reference solution for the purpose of comparisons. From this figure, it can be observed that the spike penetration converges faster towards the reference solution from the observation that the lines collapse as the mesh resolution is increased.

In order to quantify and validate this observation, we have computed an error estimate called spike penetration error. This is defined as the distance between the spike penetration for a given mesh resolution and the reference solution. This error estimate is then compared for various mesh resolutions over multiple time instants and is shown

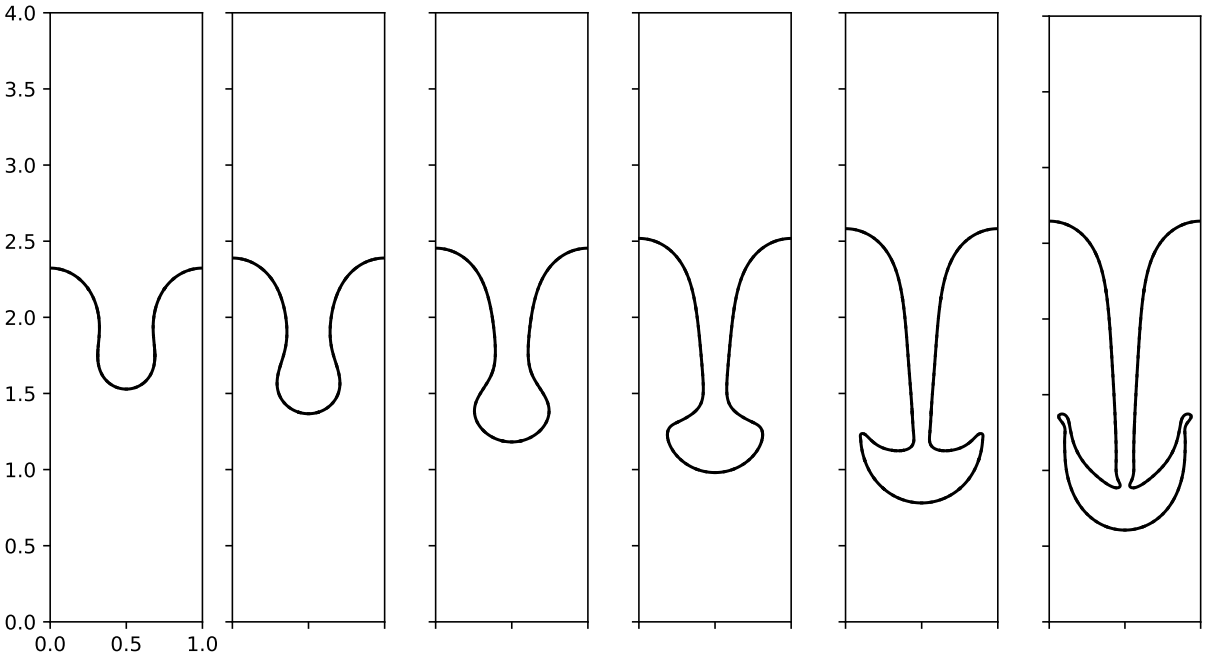

(a) $t = 0.7$ (b) $t = 0.8$ (c) $t = 0.9$ (d) $t = 1.0$ (e) $t = 1.1$ (f) $t = 1.2$

Figure 5. Time evolution of phase interface using 512×2048 mesh resolution for Rayleigh-Taylor instability using CLSMOF method.

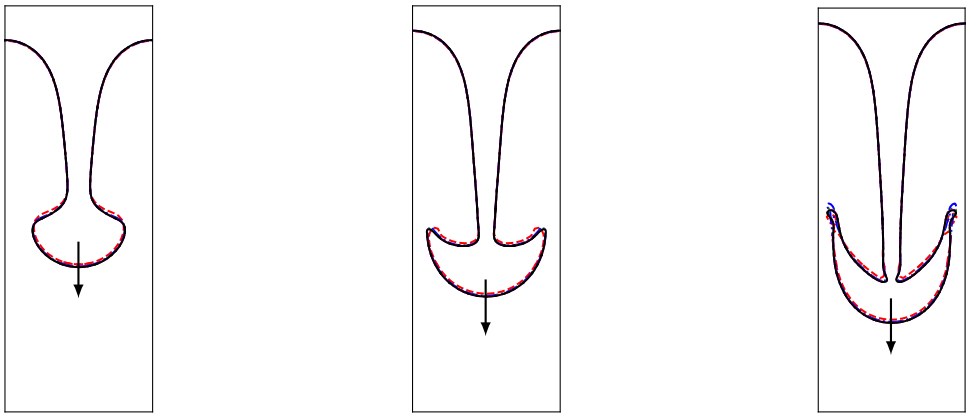

(a) $t = 1.0$ (b) $t = 1.1$ (c) $t = 1.2$

Figure 6. Fluid phase interface shape as a function of time for Rayleigh–Taylor instability test using MOF method with arrow indicating increasing mesh resolutions from 32×128 to 512×2048.

in Figure 7. A second-order convergence of the error can be observed in Figure 7 for all the three time instants which validates the observation made from Figure 6 on faster convergence. With the increasing simulation time, more complex interfacial structures such as thin filaments and ligaments are formed thereby increasing the error towards the end of the simulation.

Turbulent Atomization of Liquid Diesel Jet

Finally, we apply the CLSMOF method to simulate a more complex, turbulent, multiphase flow for diesel fuel injection using a simple round jet injector. The case setup is inspired from the work of Ménard et al [10]. In this simulation, a turbulent liquid jet of fuel is injected into a quiscent environment of gas. The jet upon penetration into the surroundings is disintegrated into ligaments and droplets upon action of shear and aerodynamic forces. To this end, we have used a domain of $24D_j \times 3D_j \times 3D_j$ that has been discretized using $1024 \times 128 \times 128$ resulting in a mesh spacing of $\Delta x = 2.36\,\mu\text{m}$. The liquid jet diameter is $D_j = 100\,\mu\text{m}$, mean liquid jet velocity $\overline{U}_j$ is $100\,\text{m/s}$, surface tension is 0.06, density ratio is 27.84 and viscosity ratio is 120 resulting in jet Reynolds number of 5800 and jet Weber number of 1.1267. The turbulent length scale has been set to 10% of the jet diameter and the turbulent intensity 5% of the mean jet velocity. The simulation has been performed for a non-dimensional time $t^* = t\overline{U}_j/D_j$

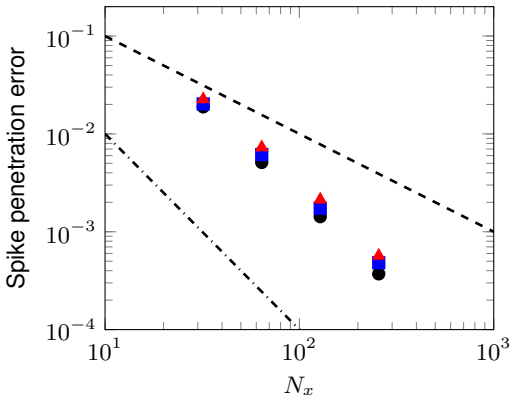

Figure 7. Error convergence plot for various mesh resolutions for Rayleigh-Taylor instability test considering 512×2048 mesh as reference solution using MOF method: $t = 1.0$ (●); $t = 1.1$ (■); $t = 1.2$ (▲); 1^{st} order convergence: (- - -); 2^{nd} order convergence: (-·-·-).

from 0 until 13.5 on 512 processors in Myria supercomputer at CRIANN supercomputing facility.

Figure 8 shows the time evolution of the liquid diesel jet with a time spacing $\Delta t^* = 3$ between each image. It can be seen that the liquid jet undergoes sever deformation thus breaking up into ligaments, sheets and finally to droplets. It is interesting to note that the jet has disintegrated into large number of ligaments and droplets at the last time step shown in this figure.

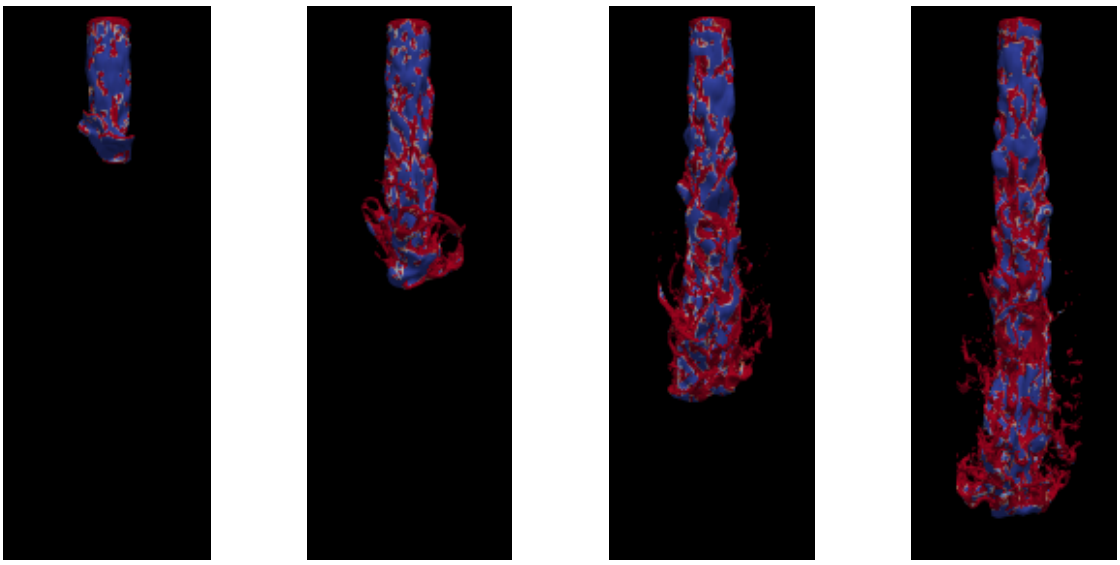

Figure 8. Turbulent atomization of liquid diesel jet. $\Delta t^* = 3$ between each image. Red regions correspond to MOF interface reconstructed regions and blue regions correspond to CLSVOF interface reconstructed regions.

The surface of the liquid jet as shown in Figure 9 has three-dimensional waves caused due to the transverse velocity gradients. These instability waves are vital in the detatchement or breakup of the liquid core of the jet into ligaments and droplets. We find three zones of instability and breakup in this jet. First zone (c.f Figure 9) is the near nozzle zone which is upto five jet diameters downstream. In this zone, we do not observe real breakup but only generation of waves on the liquid core. In the second or the transition zone, the gas enter the dense part of the liquid jet causing the waves to roll up and leading to first breakup of the liquid ligaments. The third and final zone (c.f. Figure 10) is chaotic in nature in which many ligaments and drops are ejected from the liquid core thereby leading to primary atomization.

Conclusions

A new numerical method for liquid/gas interface reconstruction called coupled level set moment of fluid (CLSMOF) method has been developed within the context of numerical simulation of multiphase flows. This method is a hybrid between conventional moment of fluid (MOF) and coupled level set volume of fluid (CLSVOF) methods. It combines the advantage of accurate capture of under-resolved liquid structures from MOF and sharp interface representation from level set function. MOF method involves solving a local non-linear optimization problem that is solved using Gauss-Newton method. This method has been demonstrated to have as high accuracy as full MOF method with less computational expense. The accuracy of this method has been assessed through tests on deformation of spherical liquid droplet and Rayleigh-Taylor instability. Finally, the usefulness of this proposed method has been shown by its

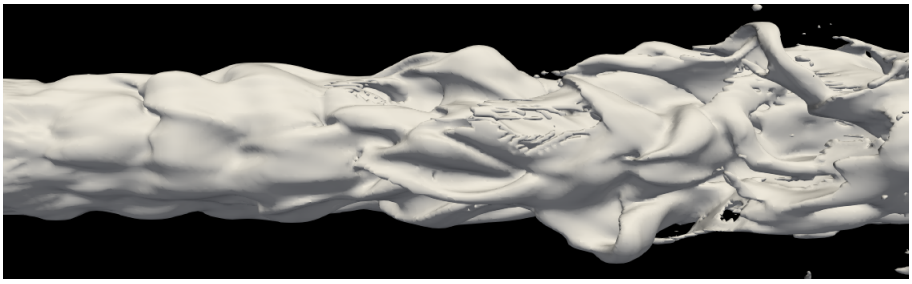

Figure 9. Surface waves on liquid jet near nozzle exit

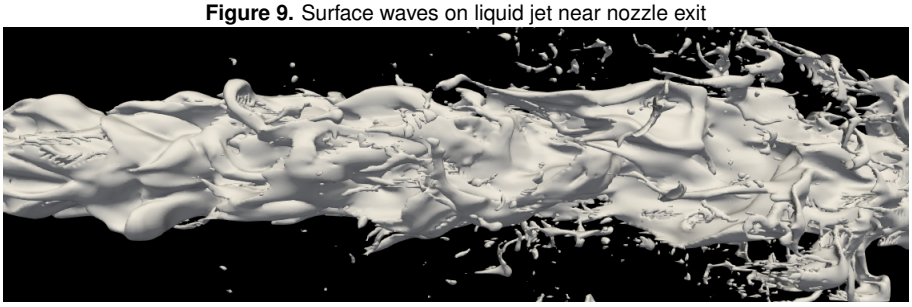

Figure 10. Detatched liquid packets from liquid jet core after breakup.

application to simulate a complex, turbulent multiphase liquid diesel injection. Three-dimensional turbulent waves are found in the jet surface that roll up causing detatchment of ligaments and droplets from the liquid core.

Acknowledgements

The funding for this project from the European Union's Horizon 2020 research and innovation programme under the Marie Skłodowska-Curie grant agreement N° 675676 is gratefully acknowledged. The computing time at CRIANN (Centre Régional Informatique et d'Applications Numériques de Normandie) under the scientific project No. 2003008 is also gratefully acknowledged.

References

[1] Gorokhovski, M. and Herrmann, M. *Annual Review of Fluid Mechanics* 40:343–366 (2008).
[2] Aulisa, E., Manservisi, S., Scardovelli, R., and Zaleski, S. *Journal of Computational Physics* 192(1):355–364 (2003).
[3] López, J., Zanzi, C., Gómez, P., Faura, F., and Hernández, J. *International Journal for Numerical Methods in Fluids* 58(8):923–944 (2008).
[4] Hernández, J., López, J., Gómez, P., Zanzi, C., and Faura, F. *International Journal for Numerical Methods in Fluids* 58:897–921 (2008).
[5] Aniszewski, W., Ménard, T., and Marek, M. *Computers & Fluids* 97:52–73 (2014).
[6] Tanguy, S. and Berlemont, A. *International Journal of Multiphase Flow* 31:1015–1035 (2005).
[7] Desjardins, O., Moureau, V., and Pitsch, H. *Journal of Computational Physics* 227:8395–8416 (2008).
[8] Herrmann, M. *Journal of Computational Physics* 227:2674–2706 (2008).
[9] Sussman, M. and Puckett, E. G. *Journal of Computational Physics* 162,:301–337 (2000).
[10] Ménard, T., Tanguy, S., and Berlemont, A. *International Journal of Multiphase Flow* 33(5):510–524 (2007).
[11] Le Chenadec, V. and Pitsch, H. *Journal of Computational Physics* 233:10–33 (2013).
[12] Dyadechko, V. and Shashkov, M. *Journal of Computational Physics* 227:5361–5384 (2008).
[13] Jemison, M., Loch, E., Sussman, M., Shashkov, M., Arienti, M., Ohta, M., and Wang, Y. *Journal of Scientific Computing* 54:454–491 (2013).
[14] Asuri Mukundan, A., Ménard, T., Berlemont, A., and Brändle de Motta, J. C. In 10th International Conference on Computational Fluid Dynamics ICCFD10 2018, 9–13 July, Barcelona, Spain (2018).
[15] Asuri Mukundan, A., Ménard, T., Berlemont, A., and Brändle de Motta, J. C. In Proceedings of the 14th ICLASS, July 22nd-26th, Chicago, USA (2018).
[16] Vaudor, G., Ménard, T., Aniszewski, W., Doring, M., and Berlemont, A. *Computers & Fluids* 152:204–216 (2017).
[17] Sussman, M., Smith, K. M., Hussaini, M. Y., Ohta, M., and Zhi-Wei, R. *Journal of Computational Physics* 221(2):469–505 (2007).
[18] Fedkiw, R., Aslam, T., Merriman, B., and Osher, S. *Journal of Computational Physics* 152(2):457–492 (1999).
[19] Weymouth, G. D. and Yue, D. K.-P. *Journal of Computational Physics* 229(8):2853–2865 (2010).
[20] Shinjo, J. and Umemura, A. *International Journal of Multiphase Flow* 36(7):513–532 (2010).
[21] Desjardins, O. and Pitsch, H. *Journal of Computational Physics* 228(5):1658–1677 (2009).